RSC Advances

PAPER

View Article Online
View Journal | View Issue

Cite this: *RSC Adv.*, 2020, **10**, 21629

A sensitive OFF–ON–OFF fluorescent probe for the cascade sensing of Al^{3+} and F^- ions in aqueous media and living cells†

Lingjie Hou,[ac] Wenting Liang,[*b] Chenhua Deng,[ac] Caifeng Zhang,[ac] Bo Liu,[d] Shaomin Shuang[b] and Yu Wang[*b]

Received 28th March 2020
Accepted 26th May 2020

DOI: 10.1039/d0ra02848g

rsc.li/rsc-advances

A simple Schiff-base ligand 2-hydroxy-1-naphthaldehyde semicarbazone (**HNS**) was synthesized and characterized. Based on the combined effect of inhibition of CH=N isomerization and chelation-enhanced fluorescence (CHEF), **HNS** functions as a fluorescence "turn on" sensor for Al^{3+} in buffered aqueous media. Based on the strong affinity of Al^{3+} to F^- ions, the *in situ* generated Al^{3+}–**HNS** complex can also be utilized as an effective chemosensor for F^- sensing by metal displacement approach, ensuing quenching of fluorescence by the reversible return of **HNS** from Al^{3+}–**HNS** complex. Thus a method using a single probe for the detection of both Al^{3+} and F^- ions is developed. The system exhibits high selectivity and sensitivity for Al^{3+} and F^- ions and the detection limits were found to be as low as 6.75×10^{-8} M and 7.89×10^{-7} M, respectively. Furthermore, the practical applicability of this probe has been examined in living cells.

1. Introduction

Aluminum is the most abundant metal in the Earth's crust and is extensively used in every sphere of life from utensils to medicine. But aluminum in excessive amounts not only hampers plant growth but damages the human nervous system and has been reported to induce Alzheimer's disease, Parkinson's disease and amyotrophic lateral sclerosis, *etc.*[1] Therefore, detection of Al^{3+} ions in natural environment and living organisms is of vital importance for human health. In this context, the development of fluorescence based probes attracted more attention because of the simplicity and high sensitivity of fluorescence assays. However, the lack of spectroscopic characteristics and poor coordination ability of Al^{3+} (ref. 2) make it very challenging to develop a highly selective sensing system for Al^{3+}.

Up to now, several fluorescent probes for Al^{3+} have been designed by various workers.[3–19] And the structures of most fluorescent probes for Al^{3+} contain nitrogen–oxygen-rich coordination environments which provide a hard-base environment for the hard-acid Al^{3+}. These probes, however, have some limitations such as poor water solubility and tedious synthetic procedure, which limited their practical applications. Thus, only few examples of Al^{3+} probes can be used for cell imaging and biological samples.[5,8,9,12–15] Overall, it is still highly desirable to develop novel fluorescent probes for Al^{3+} which satisfies several parameters *viz.* easy and economical synthetic procedure, moderate water solubility and being suitable for cell imaging studies.

Moderate fluoride for human has good performance in the treatment of osteoporosis and the prevention of dental caries. However, excess presence of for human body may lead to dental fluorosis, skeletal fluorosis, osteoporosis, and osteosclerosis.[20] Thus, the development of an efficient F^- fluorescent sensor is quite important.[21–23] Interestingly, emissive probe + Al^{3+} complexes can serve as anion sensors, especially to F^-.[24–29] And these sensors that are capable of detecting Al^{3+} and F^- sequentially by fluorescence OFF–ON–OFF signaling response are highly effective when compared with the one-to-one probes.[30–32]

With these considerations in mind, we herein report an easily synthesizable Schiff base receptor 2-hydroxy-1-naphthaldehyde semicarbazone (**HNS**), which commendably supports the idea of the sequential sensing property for Al^{3+} and F^- in aqueous media and live cells. 2-Hydroxynaphthalene was selected as a signaling moiety for its low fluorescence quantum yield,[33] short fluorescence lifetime,[34] good binding sites and low cost. The binding of Al^{3+} with the phenolic –OH group and Schiff base nitrogen atoms of **HNS** would inhibit the *cis–trans*

[a]*Department of Chemistry, Taiyuan Normal University, Jinzhong 030619, P. R. China*
[b]*Department of Chemistry, Institute of Environmental Science, Shanxi University, Taiyuan 030006, P. R. China. E-mail: liangwt@sxu.edu.cn; wangyu1168@sxu.edu.cn*
[c]*Humic Acid Engineering and Technology Research Center of Shanxi Province, Jinzhong 030619, P. R. China*
[d]*National Institutes for Food and Drug Control, Beijing 100050, P. R. of China*

† Electronic supplementary information (ESI) available: ^{1}H NMR spectrum, ^{13}C NMR spectrum and HRMS spectrum of **HNS**. Job's plot for **HNS** and Al^{3+} complexation in EtOH/H_2O. Benesi–Hildebrand plot from fluorescence titration data of **HNS** with Al^{3+}. FTIR spectra of **HNS** and Al^{3+}–**HNS** complex. ^{1}H NMR spectrum, ^{13}C NMR spectrum, and HRMS spectrum of Al^{3+}–**HNS** complex after adding F^-. See DOI: 10.1039/d0ra02848g

isomerization around C=N and increase the rigidity of the molecular assembly to produce significant fluorescence enhancement, which shows a selective sensing property for Al^{3+} in buffered aqueous media. Further, the formed Al^{3+}–**HNS** complex can be utilized for the sensitive detecting of fluoride owing to the strong binding affinity of Al^{3+} for F^- ions.[35] Hence, the gradual addition of F^- ions into a mixture of **HNS** and Al^{3+} ions releases **HNS**, and shows fluorescence quenching. Thus, a single-probe sensory system was developed to detect both Al^{3+} cation and F^- anion with good detection reversibility, which would greatly decrease the cost for detection. What's more, detection of intracellular Al^{3+} and F^- in live SiHa cells by fluorescence imaging has been demonstrated in this study.

2. Experimental

2.1 Chemicals and instrumentation

2-Hydroxy-1-naphthaldehyde (98%) was purchased from Energy Chemical (Shanghai, China). Aminourea hydrochloride was purchased from Aladdin Reagent Co. (Shanghai, China). All the other chemical reagents were of analytical grade and used as received without further purification. Stock solutions of metal ions were prepared by dissolving their nitrates in water and stock solutions of anions were prepared from the corresponding sodium salts. Hexamethylenetetramine–HCl buffer solution of pH 5.3 was prepared by mixing appropriate ratios of 0.01 mol L^{-1} hexamethylenetetramine and 0.1 mol L^{-1} HCl solutions. Double distilled water was used throughout. All the solutions have been stocked in the plastic centrifugal tubes.

The UV absorption spectra were recorded on a Puxi TU-1901 UV-vis absorption spectrophotometer (China). Fluorescence measurements were performed on a LS-55 spectrofluorimeter (PerkinElmer, USA). The samples were excited at 390 nm. The excitation and emission slits were set at 6 and 4 nm, respectively. IR spectra were taken as KBr pellets on a TENSOR II infrared spectrometer (Bruker, Germany). ^{1}H-NMR spectra were recorded on a DRX-300 spectrometer (Fällenden, Switzerland). The pH measurements were carried out on a pHS-3C acidometer (Shanghai Precision & Scientific Instrument Co., Ltd, China). High resolution mass spectra (HRMS) were obtained on a Bruker micrOTOF-Q III mass spectrometer. The fluorescence intracellular images were obtained using an Olympus FV1000 confocal microscope (Tokyo, Japan) with a 40× objective (excited at 405 nm).

2.2 Synthesis of 2-hydxoxy-1-naphthaldehyde semicarbazone (HNS)

Scheme 1 shows the facile one step synthesis of the ligand **HNS**. Aminourea hydrochloride (259 mg, 2.32 mmol) was dis-solved in 8 mL of ethanol. The solution was neutralized to pH 7.0 with 1.0 M of NaOH and then was mixed with the ethanol solution of 2-hydroxy-1-naphthaldehyde (200 mg, 1.16 mmol). The mixture was heated under reflux for 4 h and then cooled to room temperature. Saturated sodium chloride solution was added dropwise and the precipitated solid was filtered off, washed with cold water and dried under vacuum and recrystallized from ethanol to give the product as a light-yellow solid (170 mg, 64% yield). IR ν_{max} (KBr): 3450, 3350, 1670, 1602, 1431, 1189 cm^{-1}. ^{1}H NMR (DMSO-d_6) δ: 6.37 (s, 2H, NH_2), 7.20 (d, 1H, ArH), 7.34 (t, 1H, ArH), 7.52 (t, 1H, ArH), 7.85 (t, 2H, ArH), 8.38 (d, 1H, ArH), 8.86 (s, 1H, NH), 10.22 (s, 1H, CH=N), 11.24 (s, 1H, OH). ^{13}C NMR (DMSO-d_6): 161.51, 161.31, 145.24, 136.86, 136.74, 134.12, 133.38, 132.95, 128.72, 127.51, 123.87, 115.25. HRMS (ESI): calcd for $C_{12}H_{12}N_3O_2$ (**HNS** + H) 230.0930, found 230.0927.

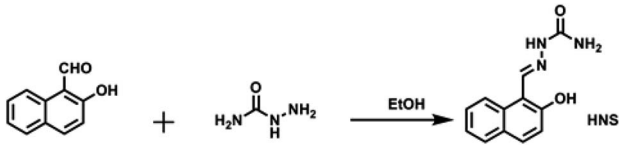

Scheme 1 The synthesis of probe **HNS**.

2.3 Cell imaging study

In vitro experiments were performed using SiHa cells. SiHa cells were cultured in DMEM medium, which was supplemented with 10% fetal bovine serum (FBS) in an atmosphere of 5% CO_2 at 37 °C. Immediately before the experiments, the cells were incubated with 50 μL **HNS** (10^{-3} M, ethanol solution) in 1 mL 0.1 M sterile PBS buffer for 30 min at room temperature. After incubation, the cells were washed with PBS buffer and incubated with Al^{3+} (100 μM) for additional 10 min at room temperature. Finally, the cells treated with **HNS** and Al^{3+} were further incubated with NaF (500 μM) for another 10 min. The fluorescence intracellular images were obtained using an Olympus FV1000 confocal microscope (Tokyo, Japan) with a 40× objective (excited at 405 nm).

3. Results and discussion

3.1 Spectral characteristics of HNS and HNS–Al^{3+}

HNS could be dissolved in water when 10% (v/v) of ethanol was added. So, the spectroscopic properties of **HNS** were investigated in an ethanol–water (1 : 9, v/v) solution at pH 5.3. As shown in Fig. 1a, the absorption spectrum of **HNS** exhibits structured absorption spectrum corresponding to the π–π* transitions of naphthalene unit observed in naphthalene derivatives.[36] Upon addition of increasing amounts of Al^{3+}, the longest-wavelength absorption band red shifted from 348 nm to 381 nm. The presence of two clear isosbestic points (330 and 363 nm) indicates the formation of a complex between **HNS** and Al^{3+}.

Fig. 1b shows the changes in the emission intensity of **HNS** upon gradual increase of [Al^{3+}]. **HNS** shows very weak broad emission in the range from 400 nm to 550 nm with a maximum at 449 nm on excitation at 390 nm. Upon addition of Al^{3+}, **HNS** shows large fluorescence enhancement, accompanied with a blue-shift of emission maxima from 449 nm to 441 nm. The results suggest that Al^{3+} most likely forms stable fluorescent complex with **HNS**. Schiff-bases usually have low emission due to the isomerization reaction around the imine linkage C=N.[37] This isomerization, however, is inhibited by the binding of Al^{3+} ions leading to fluorescence switching of the receptor. In

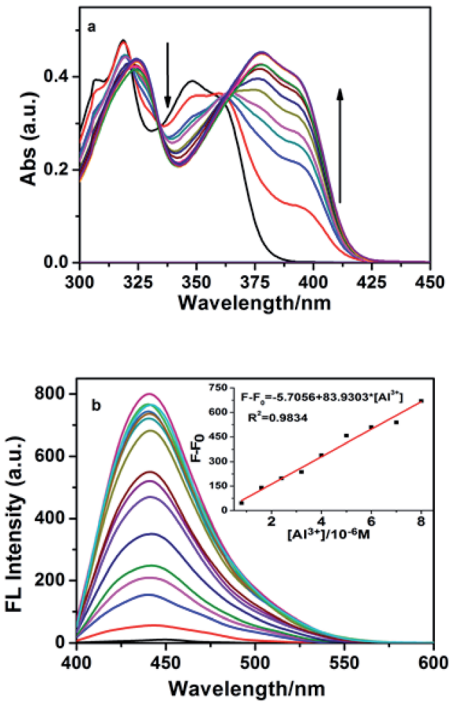

Fig. 1 (a) UV/vis spectra of **HNS** (40 μM) in the presence of different concentrations of Al^{3+} (0–10 equiv.) and (b) fluorescence titration spectra of **HNS** (4 μM) upon the addition of Al^{3+} ions (0–8 equiv.) in EtOH/H_2O (1 : 9, v/v, pH 5.3). The inset in (b) shows the fluorescence intensity of **HNS** as a function of Al^{3+} ion concentration) indicates the formation of a complex between **HNS** and Al^{3+}.

addition, the chelation of **HNS** with Al^{3+} increases the rigidity of the molecular assembly, resulting in enhancement of emission intensity ascribed as CHEF.

3.2 Fluorescence sensing of Al^{3+}

Optimization of pH on the efficiency of the sensor was essential. Fluorescence pH titrations were carried out for this purpose. Fig. 2 clearly demonstrates that at the pH range from 4.2 to 5.4, the **HNS**–Al^{3+} system showed maximum emission intensity but decrease outside this range. Most plausibly, breakage of imine linkage of **HNS** at too low pH prevents coordination of Al^{3+} while at high pH values OH^- may succeed against **HNS** in binding to

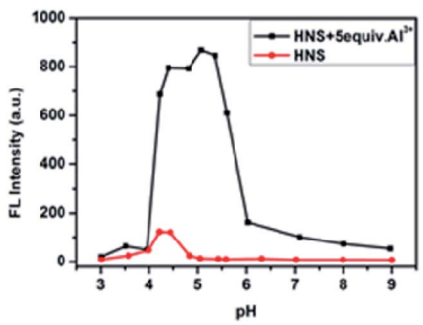

Fig. 2 Effect of pH on fluorescence intensity of the Al^{3+}–**HNS** complex in EtOH/H_2O (1 : 9, v/v), [**HNS**] = 4 μM, [Al^{3+}] = 20 μM.

Al^{3+}. In order to obtain a higher signal-to-noise, pH = 5.3 with hexamethylenetetramine–hydrochloric acid buffer solution was chosen throughout the experiment.

Selectivity of **HNS** as the fluorescence chemosensor for Al^{3+} was studied in the presence of various competing metal ions. Under the same conditions as used above for Al^{3+}, we tested the fluorescence responses of **HNS** toward other metal ions such as Pb^{2+}, Na^+, Cd^{2+}, K^+, Mg^{2+}, Cu^{2+}, Co^{2+}, Zn^{2+}, Ni^{2+}, Hg^{2+}, Ca^{2+}, Fe^{3+} and In^{3+}. As shown in Fig. 3a, significant spectral changes were observed only in the case of Al^{3+}. In contrast, treatment with other metal ions resulted in no significant changes, demonstrating that **HNS** is highly selective for Al^{3+} over competing metal ions. Furthermore, it was observed that the emission intensity of the Al^{3+}–**HNS** complex was not remarkably affected by most coexistent metal ions except Cu^{2+} and Fe^{3+} (Fig. 3b). Cu^{2+} showed complete quenching in fact, where luminescence was even less than that of **HNS** alone. A similar phenomenon was previously reported by Jang *et al.*[38] Thus **HNS** can be applied as an effective fluorescent sensor for Al^{3+} in the presence of most competing metal ions.

Based on the fluorometric spectra studies, a calibration curve was constructed by plotting the values of $F - F_0$ against Al^{3+} concentration (inset of Fig. 1b). A good linear relationship between $F - F_0$ and the concentration of Al^{3+} could be obtained in the range of 0.8–8 μM ($R^2 = 0.9834$). The limit of detection was measured to be 6.75×10^{-8} M (signal to noise ratio of 3 : 1), which is satisfactory to the Al^{3+} detection in drinking water within World Health Organization (WHO) limit (200 μg L^{-1}, 7.41 μM).[39] In terms of sensitivity, the detection limit of the proposed method is better than or comparable to those of

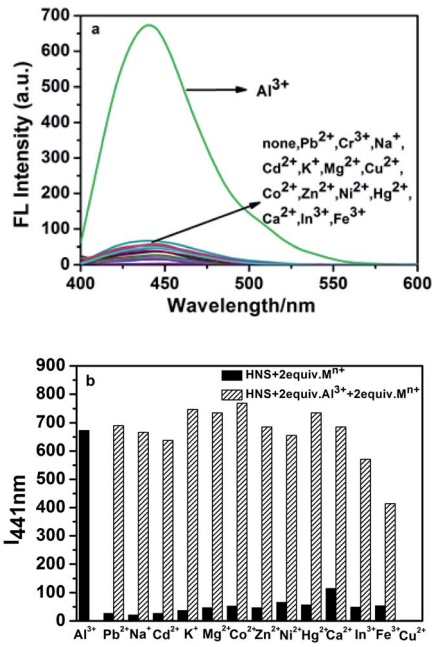

Fig. 3 (a) Fluorescence spectra changes of **HNS** (4 μM) in the presence of various metal ions (8 μM) in EtOH/H_2O (1 : 9, v/v, pH 5.3). (b) Fluorescence intensities of **HNS** (4 μM) at 441 nm ($I_{441\ nm}$) upon addition of Al^{3+} in the presence of interfered metal ions.

previously reported Schiff base probes for Al^{3+} detection.[8,9,15] The relative standard deviation for five repeated measurements of 8.0×10^{-6} M of Al^{3+} was 1.08%, which illustrated that the response of **HNS** toward Al^{3+} was highly reproducible. It should be noted that this switch on sensing process could be easily observed by the naked eye. As shown in Fig. 7, **HNS** alone only exhibited very weak fluorescence, but gave a strong blue fluorescence in the presence of Al^{3+}.

3.3 Binding mode of HNS with Al^{3+}

A Job plot obtained from emission data showed a 2 : 1 stoichiometry of the complex formed between **HNS** and Al^{3+} (Fig. S4a†), which was corroborated by the mass spectra of Al^{3+}–**HNS** complex. The HRMS spectrum showed a peak at *m*/*z* 483.1361 corresponding to 2**HNS** + Al^{3+}–$2H^+$ [calcd, *m*/*z*: 483.1345] (Fig. 4), indicating that the binding of Al^{3+} to **HNS** induced deprotonation of the phenolic –OH group of **HNS**. Based on a 2 : 1 binding mode, the association constant (*K*) was evaluated from the Al^{3+} ions titration curve (Fig. S4b†) using the modified Benesi–Hildebrand method[19] and was found to be 1.14×10^4 M^{-1}.

Further evidence for the Al^{3+} coordination was obtained from the FT-IR and NMR spectral studies. In the IR spectrum of Al^{3+}–**HNS** complex shown in Fig. S5,† the sharp peaks at 3450 cm^{-1} and 3350 cm^{-1} may be attributed to N–H stretching of $–CONH_2$ group of **HNS**. On co-ordination with Al^{3+} ions, these peaks became a broad band, indicating that the primary amide participated in the binding with Al^{3+}. In addition, the stretching vibration band of C=N at 1603 cm^{-1} shifted to a lower frequency by 31 cm^{-1}, clearly indicating the coordination of imine nitrogen atom of **HNS** to aluminium ion.

^{1}H NMR spectroscopy was used to ascertain the binding mode of **HNS** to Al^{3+}. ^{1}H NMR spectra of **HNS** were recorded in DMSO-d_6 with increasing concentrations of Al^{3+} (as its nitrate salt). Significant spectral changes were observed as shown in Fig. 5. After addition of Al^{3+}, the H_a protons of the phenolic hydroxyl progressively disappeared, suggesting the occurrence of deprotonation during the coordination to metal ions. The amino proton peak (H_b) at around 6.37 ppm became broader, indicating the coordination of the amino nitrogen to Al^{3+}. Meanwhile, the imine proton peak (H_c) at around 10.22 ppm became less intense and slightly downfield shifted by 0.02 ppm, supporting the coordination of the imine nitrogen to Al^{3+}. The overall changes in ^{1}H NMR spectra indicate the complexation between Al^{3+} and **HNS** through amino-N, azomethine-N and phenolic-OH. Based on the Job's plot, IR spectra, mass spectra and NMR titration, we proposed a rational coordinated mode that aluminium ion is hexa-coordinated with two tridentate ligand **HNS** shown in Fig. 5.

3.4 Fluorescence sensing of F^-

The sensor Al^{3+}–**HNS** for fluoride detection was prepared *in situ* by addition of 2.0 equiv. of Al^{3+} to C_2H_5OH/H_2O (1 : 9, v/v) solution of **HNS**. The F^- sensing property of Al^{3+}–**HNS** was then evaluated by fluorescence titration experiments and the results were depicted in Fig. 6. As shown in Fig. 6a, the fluorescent intensity at 441 nm can be significantly quenched by F^- ions. The quenching effect of F^- on the fluorescence emission of the system is concentration dependent. There is a good linear relationship ($R^2 = 0.9957$) between the fluorescence intensity and F^- concentration in the range of 0.8–20 μM. Thus, probe **HNS** could not only act as a sensor for Al^{3+} but also for F^- in a successive manner.

Interferences from common anions have also been studied under the same conditions as used above for F^-. Out of the tested anions, significant quenching was observed only in case of fluoride (Fig. 6b). Furthermore, the other coexistent anions had a small and negligible effect on the emission intensity of the system, suggesting the high selectivity of the Al^{3+}–**HNS** ensemble for F^- over other anions. The detection limit of Al^{3+}–**HNS** complex as a fluorescent sensor for the analysis of F^- was obtained from a plot of fluorescence intensity as a function of

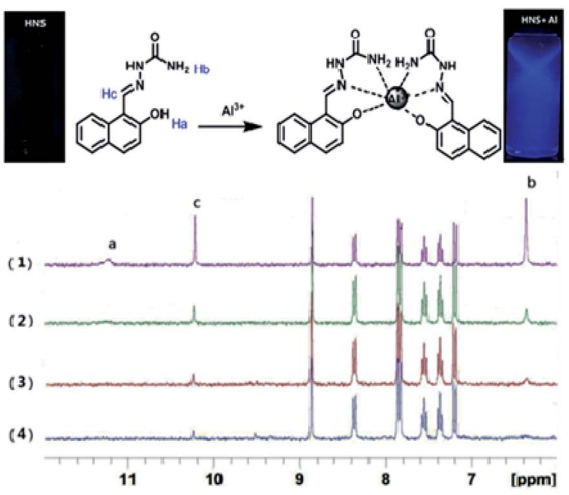

Fig. 4 The ESI-MS spectra of Al^{3+}–**HNS** complex.

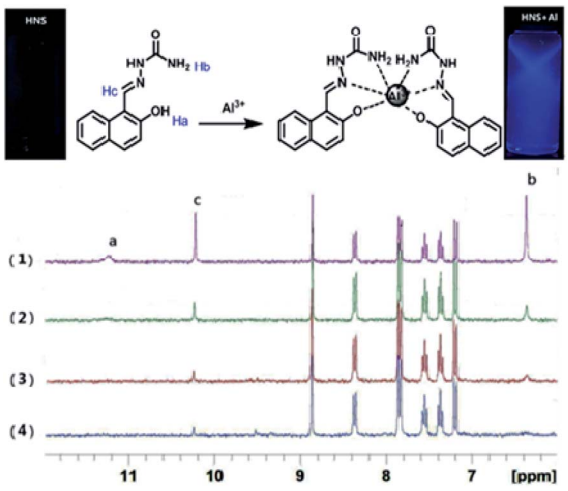

Fig. 5 Top: Binding mode of Al^{3+}–**HNS** system. Bottom: ^{1}H NMR spectra of **HNS** in the presence of different concentrations of Al $(NO_3)_3 \cdot 9H_2O$ in d_6-DMSO: (1) **HNS** only; (2) **HNS** + Al^{3+} (0.25 equiv.) and (3) **HNS** + Al^{3+} (0.5 equiv.) (4) **HNS** + Al^{3+} (1 equiv.).

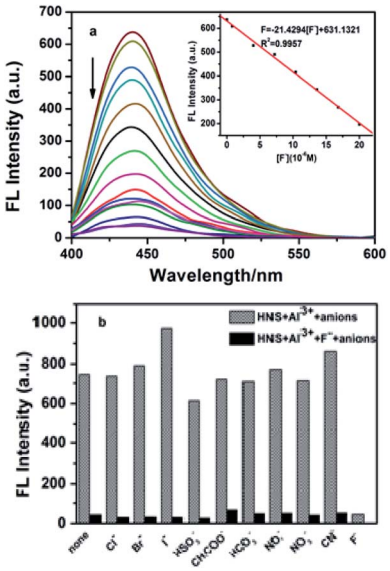

Fig. 6 (a) Fluorescent emission spectra of Al^{3+}–HNS in the presence of different concentrations of F^- in ethanol/water = 1 : 9 at pH 5.3. [HNS] = 4×10^{-6} M, [Al^{3+}] = 8×10^{-6} M, and (b) competitive signaling of fluoride ions by Al^{3+}–HNS in the absence (the twill) and presence (the black) of other anions as background in ethanol/water = 1 : 9 (pH = 5.3). [HNS] = 4×10^{-6} M, [anions] = 8×10^{-5} M.

the concentration of the different amounts of F^- added. It was found that Al^{3+}–**HNS** has a detection limit of 7.89×10^{-7} M for F^-, which is much lower than the maximum contaminant level defined by the U.S. Environmental Protection Agency (4.0 mg L^{-1}, 211 μM).[40]

This phenomenon can be supposed that the Al^{3+} has been captured by F^- ions from the [Al^{3+}–**HNS**] complex to form a new more stable complex AlF_3 and resulted in the release of free **HNS** (Scheme 2). To elucidate the nature of the strong binding of F^- to Al^{3+}, the UV-vis spectra, ^{1}H NMR spectra and HRMS experiments have been conducted respectively. As shown in Fig. 7, toward adding F^-, the characteristic band at 381 nm of [Al^{3+}–**HNS**] complex is disappeared, while the absorption response is recovered to the original state of free **HNS**. The ^{1}H NMR spectrum of [Al^{3+}–**HNS**] complex has been investigated in absence and in presence of Al^{3+} in DMSO-d_6 (Fig. S6†). The broader amino proton peak (H_b) at around 6.37 ppm became sharp and the imine proton peak (H_c) at around 10.22 ppm became recovered, indicating the dissociation of the Al^{3+} to **HNS** after adding F^-. This was further confirmed by HRMS studies of

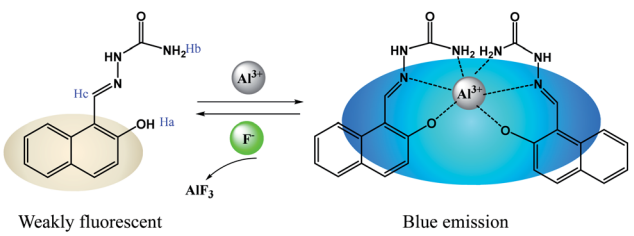

Scheme 2 Probable sensing mechanism for Al^{3+} and F^- by HNS.

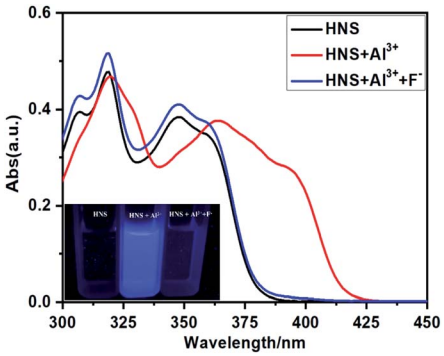

Fig. 7 UV/vis spectra of HNS (40 μM) in the presence of Al^{3+} (4 equiv.) and Al^{3+} (4 equiv.) + F^- (8 equiv.). Inset: the visual change exhibited for HNS in the presence of Al^{3+} and F^- under UV light.

HNS + $Al(NO_3)_3$ (2.0 equiv.) + NaF (8.0 equiv.) (Fig. S7†). The peak of 2**HNS** + Al^{3+}–$2H^+$ [calcd, *m/z*: 483.1345] at *m/z* = 483.1355 became very weak and the peak at *m/z* = 230.0924 corresponded to [**HNS** + H^+] (230.0930) displayed a prominent peak, which further proved that the [Al^{3+}–**HNS**] complex released the free **HNS** by addition of F^-. The overall changes in UV-vis spectra, ^{1}H NMR spectra and HRMS analysis confirmed the dissociation between Al^{3+} and **HNS**, meanwhile, indirectly demonstrated the higher binding affinity of Al^{3+} toward F^- compared to that with **HNS**.

3.5 Cellular imaging by fluorescence microscopy

To demonstrate the potential of **HNS** to image Al^{3+} in living matrices, we carried out the experiments in SiHa cells. First, an MTT assay in SiHa cells has been performed to explore the cytotoxicity of **HNS** (Fig. S8†). The result confirmed that the **HNS** has no significant cytotoxicity on SiHa cells at a low concentration. As shown in Fig. 8, the cells showed no detectable fluorescence upon incubation only with **HNS** (50 μM) for 30 min. However, bright blue fluorescence was observed after the cells were incubated with receptor **HNS** (50 μM) and Al^{3+} (100 μM) simultaneously. Cells were subsequently incubated with a 500 μM solution of F^- for 10 min under the same conditions, whereupon a significant decrease in the fluorescence was observed. During the whole process, the cells remained in good cell morphological state, demonstrating the low cytotoxicity of the probe further. These results demonstrate that **HNS** has good cell-membrane permeability and can be used for sequential detection of Al^{3+} and F^- in an *in vitro* cellular system.

4. Conclusions

In conclusion, we have developed an "off–on" type chemosensor **HNS** for Al^{3+} in weak acid aqueous solution. The receptor showed a high sensitivity for Al^{3+} detection at concentrations ranging from 0.8 μM to 8 μM with a detection limit of 67.5 nM. Moreover, fluorescence of the Al^{3+}·**HNS** complex was drastically quenched by F^- *via* Al^{3+} displacement. Thus the Al^{3+}·**HNS** ensemble represents itself as an effective chemosensor for F^-

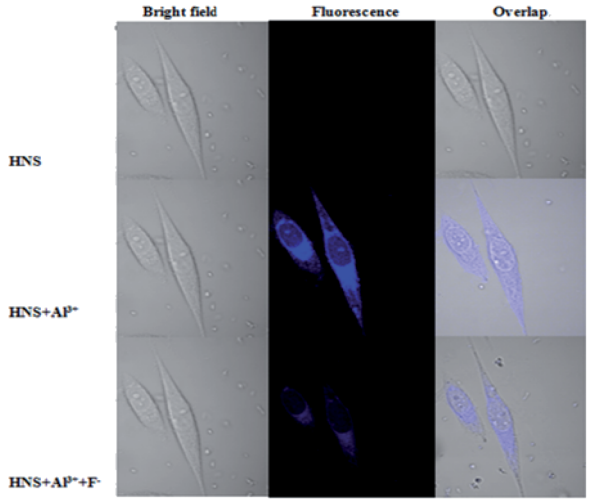

Fig. 8 Fluorescence images of SiHa cells treated with **HNS**, Al^{3+} and F^-. (Left) Bright field image; (middle) fluorescence image; (right) merged image.

too. The detection limit of F^- is quite low (0.789 μM) using this ensemble. Furthermore, **HNS** has been utilized successfully for sequential detection of Al^{3+} and F^- ions in living cells. These merits of **HNS**, *i.e.*, requiring facile one-step synthesis, working in aqueous media, possessing low detection limits, displaying high selectivity, and being suitable for monitoring Al^{3+} in living cell, make **HNS** a promising candidate as a chemosensor for Al^{3+} and F^- ions.

Conflicts of interest

There are no conflicts to declare.

Acknowledgements

This work was financially supported by the National Natural Science Foundation of China (No. 21976113), the Natural Science Foundation of Shanxi Province (No. 201801D221142, 201801D221059), the Scientific and Technologial Innovation Programs of Higher Education Institutions in Shanxi (No. 2019L0787) and Beijing Natural Science Foundation (No. 7194337).

Notes and references

1 (*a*) E. Altschuler, *Med. Hypotheses*, 1999, **53**, 22; (*b*) J. R. Walton, *NeuroToxicology*, 2006, **27**, 385; (*c*) B. Wang, W. Xing, Y. Zhao and X. Deng, *Environ. Toxicol. Pharmacol.*, 2010, **29**, 308.
2 K. Soroka, R. S. Vithanage, D. A. Phillips, B. Walker and P. K. Dasgupta, *Anal. Chem.*, 1987, **59**, 629.
3 A. Gupta and N. Kumar, *RSC Adv.*, 2016, **6**, 106413.
4 D. Kara, A. Fisher and S. J. Hill, *J. Environ. Monit.*, 2007, **9**, 994.
5 Z. Liu, S. Li, G. Ge, Y. Li, C. Zhao, H. Zhang and Z. Yang, *RSC Adv.*, 2019, **9**, 5377.
6 Y. Lu, S. S. Huang, Y. Y. Liu, S. He, L. C. Zhao and X. S. Zeng, *Org. Lett.*, 2011, **13**, 5274.
7 D. Maity and T. Govindaraju, *Chem. Commun.*, 2012, **48**, 1039.
8 S. Sen, T. Mukherjee, B. Chattopadhyay, A. Moirangthem, A. Basu, J. Marek and P. Chattopadhyay, *Analyst*, 2012, **137**, 3975.
9 A. Sahana, A. Banerjee, S. Das, S. Lohar, D. Karak, B. Sarkar, S. K. Mukhopadhyay, A. K. Mukherjee and D. Das, *Org. Biomol. Chem.*, 2011, **9**, 5523.
10 L. Cao, C. Jia, Q. Zhang, D. Chen, C. Zhang and Y. Qian, *Chem. Res. Chin. Univ.*, 2014, **30**(3), 362.
11 Y. Wang, L. J. Hou, Y. B. Wu, L. L. Shi, Z. B. Shang and W. J. Jin, *J. Photochem. Photobiol., A*, 2014, **281**, 40.
12 Y. P. Dai, X. Y. Liu, P. Wang, J. X. Fu, K. Yao and K. X. Xu, *RSC Adv.*, 2016, **6**, 99933.
13 Q. Jiang, M. X. Li, J. Song, Y. Q. Yang, X. Xu, H. J. Xu and S. F. Wang, *RSC Adv.*, 2019, **9**, 10414.
14 H. H. Wang, B. Wang, Z. H. Shi, X. L. Tang, W. Dou, Q. X. Han, Y. G. Zhang and W. S. Liu, *Biosens. Bioelectron.*, 2015, **65**, 91.
15 S. K. Sheet, B. Sen, R. Thounaojam, K. Aguan and S. Khatua, *J. Photochem. Photobiol., A*, 2017, **332**, 101.
16 Y. J. Liu, F. F. Tian, X. Y. Fan, g F. L. Jian and Y. Liu, *Sens. Actuators, B*, 2017, **240**, 916.
17 G. Kumar, K. Paul and V. Luxami, *Sens. Actuators, B*, 2018, **263**, 585.
18 X. J. Sun, Y. Q. Ma, H. Fu, Z. Y. Xing, Z. G. Sun, Y. Shen and J. L. Li, *J. Fluoresc.*, 2019, **29**, 577.
19 J. C. Qin, T. R. Li, B. D. Wang, Z. Y. Yang and L. Fan, *Spectrochim. Acta, Part A*, 2014, **133**, 38.
20 A. Amalraj and A. Pius, *J. Fluorine Chem.*, 2015, **178**, 73.
21 L. Tang, G. Y. Zhao, Z. L. Huang, N. N. Wang and J. J. Guo, *Chem. Res. Chin. Univ.*, 2013, **29**(2), 214.
22 M. Bineci, M. Bağlan and S. Atılgan, *Sens. Actuators, B*, 2016, **222**, 315.
23 Y. Wang, Y. F. Song, L. Zhang, G. G. Dai, R. F. Kang, W. N. Wu, Z. H. Xu, Y. C. Fan and L. Y. Bian, *Talanta*, 2019, **203**, 178.
24 X. Y. Sun, L. L. Wu, J. S. Shen, X. G. Cao, C. Wen, B. Liu and H. Q. Wang, *RSC Adv.*, 2016, **6**, 97346.
25 D. Romi, D. P. Singh, B. S. Chauhan, S. Srikrishna, A. K. Panday, L. H. Choudhury and V. P. Singh, *Sens. Actuators, B*, 2018, **258**, 881.
26 X. Y. Kong, L. J. Hou, X. Q. Shao, S. M. Shuang, Y. Wang and C. Dong, *Spectrochim. Acta, Part A*, 2019, **208**, 131.
27 J. X. Fu, B. Li, H. H. Mei, Y. X. Chang and K. X. Xu, *Spectrochim. Acta, Part A*, 2020, **227**, 117678.
28 S. D. Hiremath, R. U. Gawas, S. C. Mascarenhas, A. Ganguly, M. Banerjee and A. Chatterjee, *New J. Chem.*, 2019, **43**, 5219.
29 R. Purkait, C. Patra, A. D. Mahapatra, D. Chattopadhyay and C. Sinha, *Sens. Actuators, B*, 2018, **257**, 545.
30 Y. W. Liu, C. H. Chen and A. T. Wu, *Analyst*, 2012, **137**, 5201.
31 S. M. Basheer, J. Haribabu, N. S. P. Bhuvanesh, R. Karvembu and A. Sreekanth, *J. Mol. Struct.*, 2017, **1145**, 347.
32 C. L. Li, P. H. Lu, S. F. Fu and A. T. Wu, *Sensors*, 2019, **19**, 623.
33 F. P. Schwarz and S. P. Wasik, *Anal. Chem.*, 1976, **48**, 524.

34 D. P. Roek, J. E. Chateauneuf and J. F. Brennecke, *Ind. Eng. Chem. Res.*, 2000, **39**, 3090.
35 R. B. Martin, *Chem. Rev.*, 1996, **141**, 23.
36 R. Azadbakht and S. Rashidi, *Spectrochim. Acta, Part A*, 2014, **127**, 329–334.
37 (*a*) J. S. Wu, W. M. Liu, X. Q. Zhuang, F. Wang, P. F. Wang, S. L. Tao, X. H. Zhang, S. K. Wu and S. T. Lee, *Org. Lett.*, 2007, **9**, 33; (*b*) D. Ray and P. K. Bharadwaj, *Inorg. Chem.*, 2008, **47**, 2252; (*c*) H. Y. Li, S. Gao and Z. Xi, *Inorg. Chem. Commun.*, 2009, **12**, 300; (*d*) W. M. Liu, L. W. Xu, R. L. Sheng, P. F. Wang, H. P. Li and S. K. Wu, *Org. Lett.*, 2007, **9**, 3829; (*e*) L. Li, Y. Q. Dang, H. W. Li, B. Wang and Y. Q. Wu, *Tetrahedron Lett.*, 2010, **51**, 618.
38 Y. K. Jang, U. C. Nam, H. L. Kwon, I. H. Hwang and C. Kim, *Dyes Pigm.*, 2013, **99**, 6.
39 X. Y. Shi, H. Wang, T. Y. Han, X. Feng, B. Tong, J. B. Shi, J. G. Zhi and Y. P. Dong, *J. Mater. Chem.*, 2012, **22**, 19296.
40 R. J. Carton, *Fluoride*, 2006, **39**(3), 163.